



November 2003

U.S. Navy sources and receivers for studying acoustic propagation and climate change in the ocean (L)

John L. Spiesberger

University of Pennsylvania, johnsr@sas.upenn.edu

Follow this and additional works at: http://repository.upenn.edu/ees_papers

Recommended Citation

Spiesberger, J. L. (2003). U.S. Navy sources and receivers for studying acoustic propagation and climate change in the ocean (L). Retrieved from http://repository.upenn.edu/ees_papers/8

Copyright ASA. Reprinted from *Journal of the Acoustical Society of America*, Volume 114, Issue 5, November 2003, pages 2557-2560.
Publisher URL: <http://dx.doi.org/10.1121/1.1619983>

This paper is posted at ScholarlyCommons. http://repository.upenn.edu/ees_papers/8
For more information, please contact libraryrepository@pobox.upenn.edu.

U.S. Navy sources and receivers for studying acoustic propagation and climate change in the ocean (L)

Abstract

Sounds from a U.S. Navy SSQ-110A source are received at high signal-to-noise ratios at ocean-basin scales at two Sound Surveillance Systems in the Pacific. The sounds have sufficient pulse resolution to study climatic variations of temperature. The acoustic data can be understood using ray and parabolic approximations to the wave equation. Modeled internal waves decrease pulse resolution from 0.01 to 0.1 s, consistent with observations.

Comments

Copyright ASA. Reprinted from *Journal of the Acoustical Society of America*, Volume 114, Issue 5, November 2003, pages 2557-2560 .

Publisher URL: <http://dx.doi.org/10.1121/1.1619983>

U.S. Navy sources and receivers for studying acoustic propagation and climate change in the ocean (L)

John L. Spiesberger^{a)}

Department of Earth and Environmental Science, 240 South 33rd Street, University of Pennsylvania, Philadelphia, Pennsylvania 19104-6316

(Received 13 February 2003; revised 24 July 2003; accepted 25 August 2003)

Sounds from a U.S. Navy SSQ-110A source are received at high signal-to-noise ratios at ocean-basin scales at two Sound Surveillance Systems in the Pacific. The sounds have sufficient pulse resolution to study climatic variations of temperature. The acoustic data can be understood using ray and parabolic approximations to the wave equation. Modeled internal waves decrease pulse resolution from 0.01 to 0.1 s, consistent with observations. © 2003 Acoustical Society of America. [DOI: 10.1121/1.1619983]

Pages: 2557–2560

PACS numbers: 43.30.Qd, 43.30.Re, 43.30.Pc [RAS]

I. INTRODUCTION

Sounds from explosive sources in the ocean have been identified over long distances using rays since the 1940s.¹ Such sources have been used to study acoustic propagation and to aid in locating underwater volcanoes² and missiles that fall into the sea.³ Electronically controlled sources and the U.S. Navy's Sound Surveillance System (SOSUS) have been used to study climatic changes of temperature in the ocean.^{4–6} However, scientists may not be able to afford to deploy enough sources to resolve many important climatic variations by means of tomography with the available number of SOSUS stations.⁷ This paper demonstrates that explosive sources from routine U.S. Navy operations generate sufficiently loud sounds at basin scales so that temporally resolved echoes can be identified using established models for sound speed fields and acoustic propagation. These kinds of data could be used to see if climatic temperature variations could be detected by means of tomography.

II. DATA

A source (SSQ-110A) was detonated at 23.589°N 208.717°E on 13 November 1997 (Fig. 1). Signals were received on two of the nine SOSUS stations shown in Fig. 1 of Ref. 4 at distances between 1000 and 3000 km. The location and time of the detonation were known within a few kilometers and a few seconds, respectively. Many pulses arrived at the receivers with high signal-to-noise ratios in a band from about 50 to 200 Hz (Fig. 2).

III. MODELS

Vertical profiles of sound speed are computed along geodesics using Del Grosso's algorithm⁸ and Levitus' climatological averages⁹ of temperature and salinity for Fall. The depth of minimum speed varies from 760 m at the source to 500 and 600 m, respectively, at receivers one and two. Sound speeds are transformed to Cartesian coordinates via the Earth flattening transformation.

Some of the models incorporate sound speed fluctuations obeying a Garrett–Munk spectrum of internal waves.¹⁰ These fluctuations are added to the climatological field described above. Internal wave modes are computed at range intervals of 80 km to account for changes in water depth, buoyancy frequency, and sound speed. The vertical displacements of these modes are set to zero at the surface and bottom. For each 80-km interval, a three-dimensional field of internal waves is computed in a box of 80 km by 80 km by D m where D is the average depth of the ocean in that interval. A vertical slice through the box gives the vertical displacements along the geodesic. Internal wave energy is given the standard value¹⁰ which worked before¹¹ though controversy exists.^{12–14} Remaining details for constructing internal waves follow Ref. 11 exactly.

The c_0 insensitive parabolic approximation¹⁵ is used to compute a two-dimensional field of sound along a geodesic from 0- to 8000-m depth. Travel times of pulses are computed with an accuracy of a few milliseconds.¹⁵ The field is modeled at each of 1024 acoustic frequencies from 50 to 150 Hz. The impulse response is synthesized with an inverse Fourier transform resulting in a time series with a period of 10.24 s. Near regions where the sound interacts with the bottom, the computational grid has an interval of 25 m in range and 3.9 m in depth. In other regions, the intervals are 100 m in range in 7.8 m in depth. These values are sufficient to obtain convergence within a few decibels.

Fans of rays are traced using a program, zray, that is a modification of ray.¹⁶ Eigenrays are found using another program. These programs have been used to identify acoustic paths before.¹⁷ Rays reflect specularly from the bottom. Both geometric and nongeometric arrivals are found. Nongeometric arrivals are those that provide energy at the receiver on the shadow sides of caustics. The contribution from a caustic at any angle is included if it is within 1000 m of the receiver's depth at the receiver's range. For lack of a more reliable value, rays that reflect from the bottom suffer an attenuation of 3 dB per bounce.

IV. IDENTIFYING ACOUSTIC PATHS

As shown below, the most reliable models use the parabolic approximation and Levitus' climatology⁹ with a spec-

^{a)}Electronic mail: johnsr@sas.upenn.edu

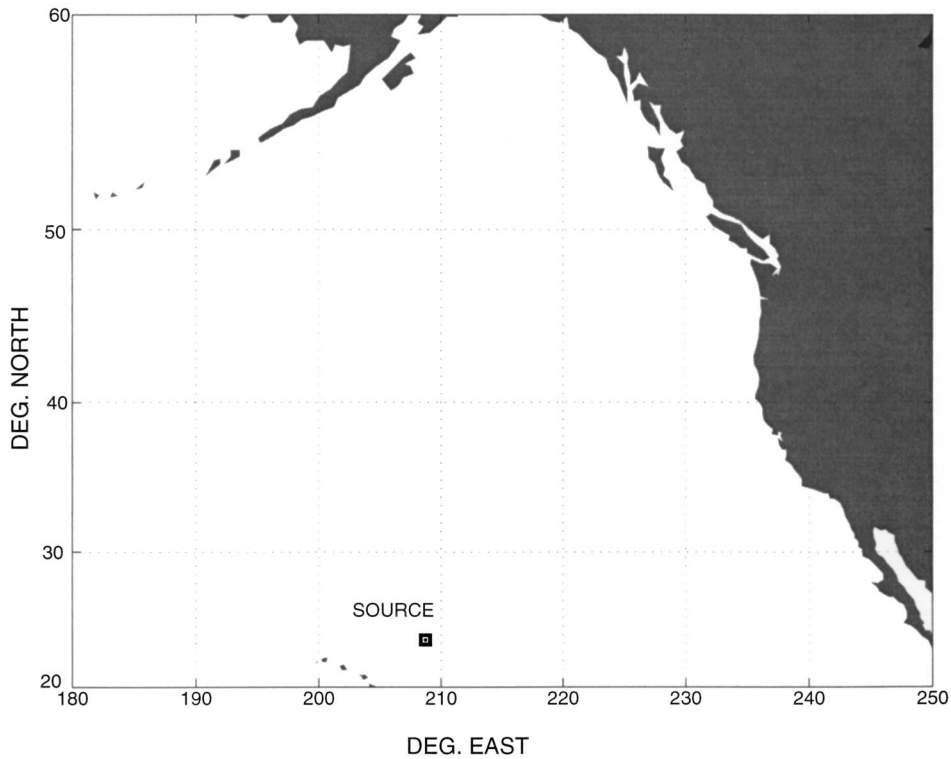


FIG. 1. The explosive source used in this experiment is an SSQ-110A. It is used in normal U.S. Navy operations. Signals are received at two of the nine Sound Surveillance Systems (SOSUS) shown in Fig. 1 of Ref. 4.

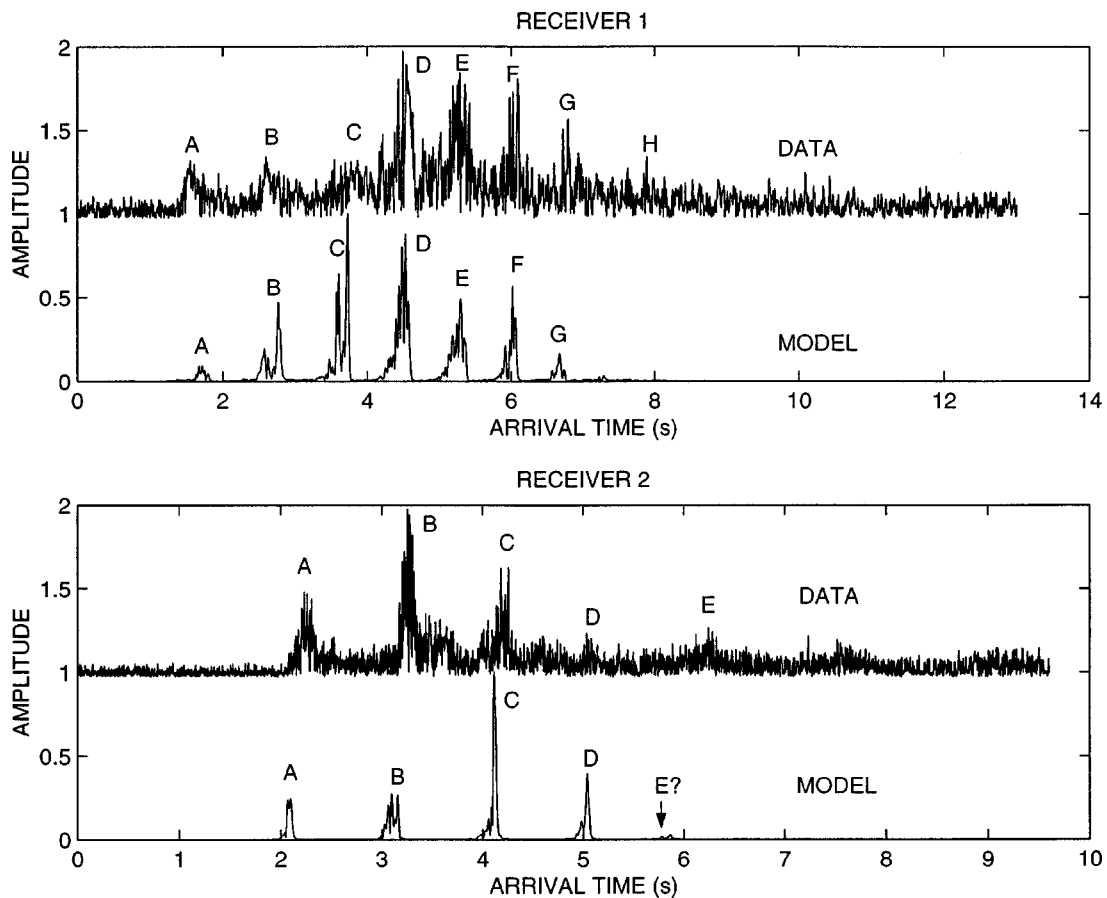


FIG. 2. Comparison of data with models at both receivers. A constant arrival time is added to the model to align with the data and a value of about one is added to the amplitudes of the data so they do not overlap. Models are computed using the c_0 insensitive parabolic approximation¹⁵ and a Garrett–Munk¹⁰ spectrum of internal waves superimposed on Levitus' climatological average conditions for Fall.⁹ Top: Arrivals except for H are predicted by the model. Bottom: Arrivals except for perhaps E are predicted by the model. Note the time scale differs from the top panel.

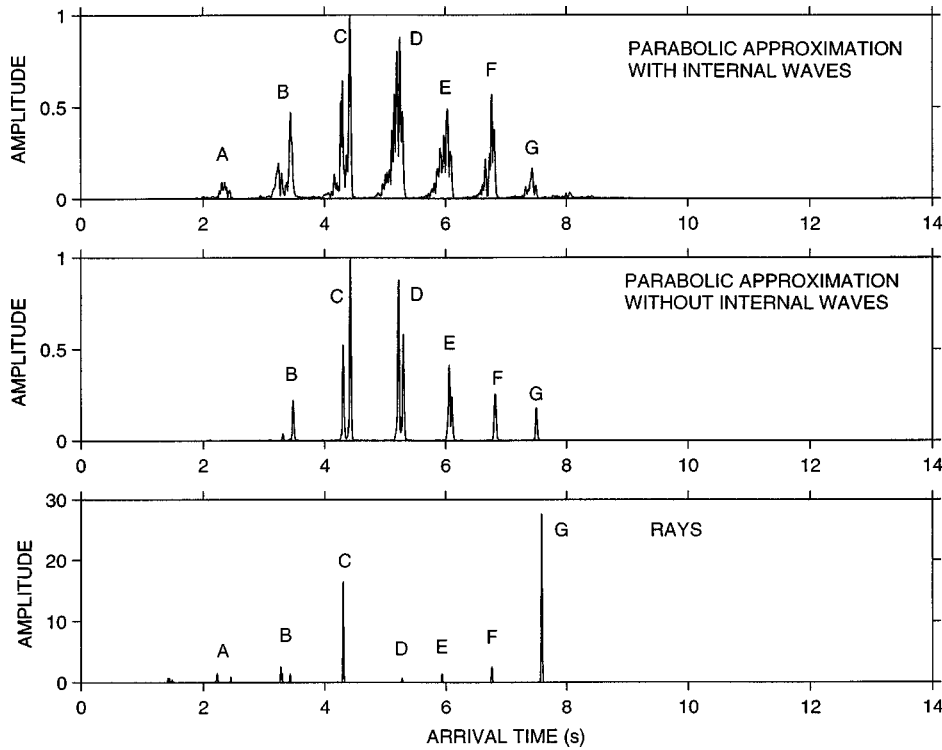


FIG. 3. Three models for the acoustic data at receiver 1. The top two models use the c_0 insensitive parabolic approximation¹⁵ with and without a spectrum of internal waves.¹⁰ The ray model uses the same sound speed field as the parabolic approximation without internal waves on the computational grid used by the parabolic approximation. Arrivals A–G are the same as Fig. 2 (top). Travel times of all three models are shifted by identical amounts so that travel times between models can be compared. Amplitudes from the parabolic approximation are normalized to unity. Amplitudes from the ray model are unnormalized.

trum of internal waves¹⁰ (Fig. 2). At receiver one, arrivals A–G appear in the data and model. The last arrival at H is not in the model. At receiver two, arrivals A–D appear in the data and model. The last arrival at E is probably not in the model. Except for the last arrivals, the relative travel times in the models resemble the data. None of the rays reflect from the bottom or surface.

The received pulses have widths from 0.1 to 0.2 s, similar to those modeled. Since the bandwidth of the model is

100 Hz, the emitted width is $1/(100 \text{ Hz}) = 0.01 \text{ s}$. This is ten times too small. Internal waves are responsible for the broadening to 0.1 s at both receivers (Figs. 3 and 4).

The correspondence between the arrival times of the data and ray models is good (Figs. 3 and 4). However, the relative amplitudes from rays are much less reliable than those from the parabolic approximation.

Arrival A at receiver one appears in the parabolic ap-

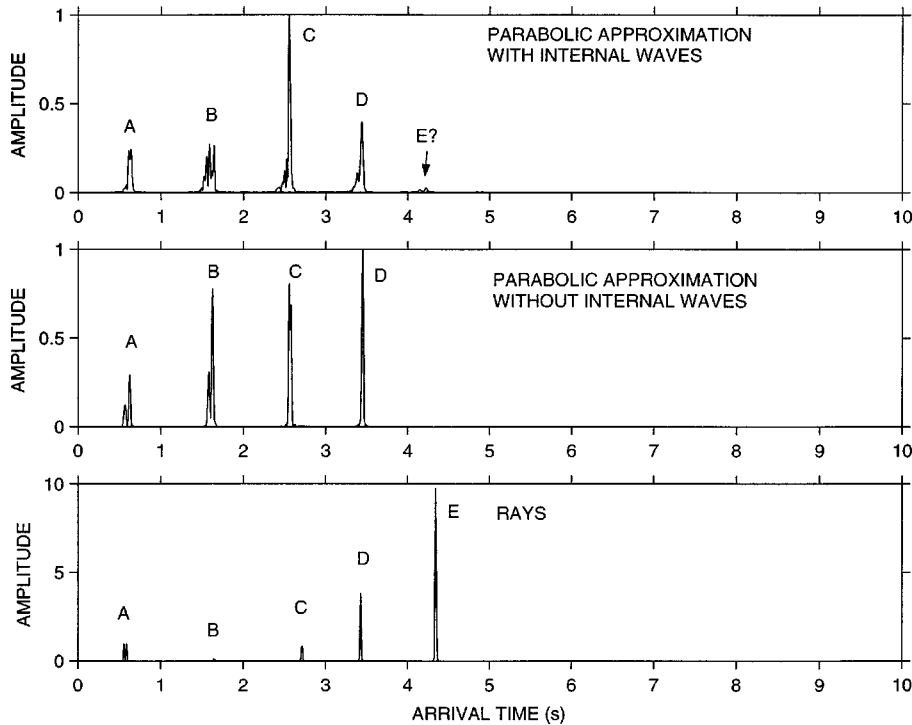


FIG. 4. Three models for the acoustic data at receiver 2. The top two models use the c_0 insensitive parabolic approximation¹⁵ with and without a spectrum of internal waves,¹⁰ respectively. The ray model uses the same sound speed field as the parabolic approximation without internal waves on the computational grid used by the parabolic approximation. Arrivals A–E are the same as the bottom panel of Fig. 2. Travel times of all three models are shifted by identical amounts so that travel times between models can be compared. Amplitudes from the parabolic approximation are normalized to unity. Amplitudes from the ray model are unnormalized.

proximation with internal waves (Fig. 3). These waves scatter the sound down to the depth of the receiver. Without scattering, the caustic from arrival *A* is too far above the receiver to detect an arrival in the parabolic approximation. The ray model yields arrival *A* without scattering because amplitudes from the ray model are not as reliable.

At receiver one, the rays have upper turning depths of about 100 to 400 m near the source. Some rays have upper turning depths near the surface at the receiver. At receiver two, upper turning depths are about 50 to 400 m near the source and receiver. As has been noted in other experiments, the rays composing each arrival have slightly different turning depths and quite different turning ranges.^{14,17,18}

V. CONCLUSION

Sounds from U.S. Navy operations can be identified with ray and parabolic approximations of the wave equation over basin-scales at Sound Surveillance stations. The fidelity is adequate for detecting climatic changes of about 1 s from El Niño and the Southern Oscillation.⁷ The next step involves a tomographic inversion to estimate the accuracy with which temperature variations are estimated at climatic scales given the navigational [$O(1)$ km] and timing uncertainties [$O(1)$ s] associated with the source. Models^{19–21} indicate that climatic signals can be detected in the presence of these errors. An experimental demonstration is needed.

Although success has been had using rays to identify paths over basin-scales in the ocean,^{4,22–24} it appears that the relative amplitudes of the arrivals are estimated with better accuracy from a parabolic approximation¹¹ and a field of internal waves.¹⁰ This field spreads the pulse resolution from ideal values of about 0.01 s to 0.1 to 0.2 s as observed.

Neither the ray nor parabolic approximations of the wave equation yield the last arrival at either receiver (Figs. 2–4), even with a realistic spectrum of internal waves. A similar problem was solved in another experiment by including a realistic mesoscale.¹¹ There, the mesoscale created a bias of about +0.6 s for sounds traveling near the depths of minimum speed in the waveguide.

ACKNOWLEDGMENTS

This research was supported by the Office of Naval Research contract N00014-00-C-0317. I thank CDR Rick Shema, (Retired) for providing the data, John Tralies (Naval Air Warfare Center, Patuxent River, MD) for answers to many questions, Bruce Einfalt and Carter Ackerman (Penn State) for computer software, and the reviewers.

¹M. Ewing and J. L. Worzel, “Long-range sound transmission,” in *Propagation of Sound in the Ocean* (Geological Society of America, New York, 1948), Memoir 27, Chap. 3, pp. 1–35.

²R. H. Johnson, “Synthesis of point data and path data in estimating sofar speed,” *J. Geophys. Res.* **74**, 4559–4570 (1969).

³G. R. Hamilton, “Time variations of sound speed over long paths in the ocean,” in *International Workshop on Low-frequency Propagation and Noise*, Woods Hole, MA (1977), Vol. 1, pp. 7–30.

⁴J. L. Spiesberger and K. Metzger, “Basin scale ocean monitoring with acoustic thermometers,” *Oceanography* **5**, 92–98 (1992).

⁵ATOC Consortium (A. B. Baggeroer, T. G. Birdsall, C. Clark, J. A. Colosi, B. D. Cornuelle, D. Costa, B. D. Dushaw, M. Dzieciuch, A. M. G. Forbes, C. Hill, B. M. Howe, J. Marshall, D. Menemenlis, J. A. Mercer, K. Metzger, W. Munk, R. C. Spindel, D. Stammer, P. F. Worcester, and C. Wunsch), “Ocean climate change: Comparison of acoustic tomography, satellite altimetry, and modeling,” *Science* **281**, 1327–1332 (1998).

⁶P. N. Mikhalevsky, A. Gavrilov, A. B. Baggeroer, and M. Slavinsky, “Experiment tests use of acoustics to monitor temperature and ice in Arctic ocean,” *EOS Trans. Am. Geophys. Union* **76**, No. 27 (1995).

⁷J. L. Spiesberger, H. E. Hurlburt, M. Johnson, M. Keller, S. Meyers, and J. J. O’Brien, “Acoustic thermometry data compared with two ocean models: The importance of Rossby waves and ENSO in modifying the ocean interior,” *Dyn. Atmos. Oceans* **26**, 209–240 (1998).

⁸V. A. Del Grosso, “New equation for the speed of sound in natural waters with comparisons to other equations,” *J. Acoust. Soc. Am.* **56**, 1084–1091 (1974).

⁹S. Levitus, “Climatological atlas of the world ocean,” in NOAA Prof. Pap. 13. U.S. Government Printing Office, Washington, DC, 1982.

¹⁰C. Garrett and W. Munk, “Space-time scales of internal waves,” *Geophys. Fluid Dyn.* **2**, 225–264 (1972).

¹¹M. A. Wolfson and J. L. Spiesberger, “Full wave simulation of the forward scattering of sound in a structured ocean: A comparison with observations,” *J. Acoust. Soc. Am.* **106**, 1293–1306 (1999).

¹²J. A. Colosi, E. K. Scheer, S. M. Flatte, B. D. Cornuelle, M. A. Dzieciuch, W. H. Munk, P. F. Worcester, B. M. Howe, J. A. Mercer, R. C. Spindel, K. Metzger, T. G. Birdsall, and A. B. Baggeroer, “Comparisons of measured and predicted acoustic fluctuations for a 3250-km propagation experiment in the eastern North Pacific Ocean,” *J. Acoust. Soc. Am.* **105**, 3202–3218 (1999).

¹³S. M. Flatte, J. A. Colosi, M. A. Dzieciuch, and P. F. Worcester, “Acoustic observations of internal-wave strength in the Mid-Pacific in 1989 and 1996,” *J. Acoust. Soc. Am.* **100**, 2582 (1996).

¹⁴F. Tappert, J. L. Spiesberger, and L. Boden, “New full-wave approximation for ocean acoustic travel time predictions,” *J. Acoust. Soc. Am.* **97**, 2771–2782 (1995).

¹⁵J. B. Bowlin, J. L. Spiesberger, T. F. Duda, and L. E. Freitag, Ocean acoustical ray-tracing software RAY, Woods Hole Oceanographic Technical Report, WHOI-93-10 (1993).

¹⁶J. L. Spiesberger and F. D. Tappert, “Kaneohe acoustic thermometer further validated with rays over 3700 km and the demise of the idea of axially trapped energy,” *J. Acoust. Soc. Am.* **99**, 173–184 (1996).

¹⁷J. Simmen, S. M. Flatte, and G. Wang, “Wavefront folding, chaos, and diffractions for sound propagation through ocean internal waves,” *J. Acoust. Soc. Am.* **102**, 239–255 (1997).

¹⁸J. L. Spiesberger, “Ocean acoustic tomography: travel-time biases,” *J. Acoust. Soc. Am.* **77**, 83–100 (1985).

¹⁹A. Fabrikant, J. L. Spiesberger, A. Silivra, and H. E. Hurlburt, “Estimating Climatic Temperature Change in the Ocean with Synthetic Acoustic Apertures,” *IEEE J. Ocean. Eng.* **23**(1), 20–25 (1998).

²⁰J. L. Spiesberger, A. Fabrikant, A. Silivra, and H. E. Hurlburt, “Mapping Climatic Temperature Changes in the Ocean with Acoustic Tomography: Navigational Requirements,” *IEEE J. Ocean. Eng.* **22**(1), 128–142 (1997).

²¹A. Silivra, J. L. Spiesberger, A. Fabrikant, and H. E. Hurlburt, “Acoustic tomography at basin-scales and clock errors,” *IEEE J. Ocean. Eng.* **22**(1), 143–150 (1997).

²²J. L. Spiesberger, T. G. Birdsall, K. Metzger, R. A. Knox, C. W. Spofford, and R. C. Spindel, “Measurements of Gulf Stream meandering and evidence of seasonal thermocline development using long range acoustic transmissions,” *J. Phys. Oceanogr.* **13**, 1836–1846 (1983).

²³D. E. Norris, J. L. Spiesberger, and D. W. Merdes, “Comparison of basin-scale acoustic transmissions with rays and further evidence for a structured thermal field in the northeast Pacific,” *J. Acoust. Soc. Am.* **103**, 182–194 (1998).

²⁴B. D. Dushaw, B. M. Howe, J. A. Mercer, R. C. Spindel, and the ATOC Group (A. B. Baggeroer, T. G. Birdsall, C. Clark, J. A. Colosi, B. D. Cornuelle, D. Costa, B. D. Dushaw, M. Dzieciuch, A. M. G. Forbes, B. M. Howe, D. Menemenlis, J. A. Mercer, K. Metzger, W. H. Munk, R. C. Spindel, P. F. Worcester, and C. Wunsch), “Multimegameter-range acoustic data obtained by bottom-mounted hydrophone arrays for measurement of ocean temperature,” *IEEE J. Ocean. Eng.* **24**, 203–214 (1999).